

Deposit Growth in the Wetting of an Angular Region with Uniform Evaporation

Rui Zheng,* Yuri O. Popov, and Thomas A. Witten
University of Chicago, Chicago, IL 60637, USA[†]
(Dated: May 9, 2019)

Solvent loss due to evaporation in a drying drop can drive outward flows and solute migration. The whole process is characterized by the evaporation rate, as well as the geometrical restriction. In this paper, as a continuation of earlier investigations [5, 6], we consider a simplified, yet physically feasible model, with uniform evaporation. We study the flow velocity field near the singularity of the angular region, and find the rate of the deposit growth along contact lines in early and intermediate time regimes. Compared to the diffusion-controlled evaporation profile, uniform evaporation yields more singular deposition at early time regime, and nearly uniform deposition profile is obtained for a wide range of opening angles in the intermediate time regime. Uniform evaporation also shows a more pronounced contrast between acute opening angles and obtuse opening angles.

PACS numbers: 47.55.Dz, 68.03.Fg, 81.15.-z

I. INTRODUCTION

Evaporative deposition, the “coffee-drop effect” has been the subject of several recent papers [1, 2, 3, 4, 5, 6, 7]. The physical problem originates from a simple phenomenon of everyday life: when a coffee drop dries on a surface, the remaining residue forms a characteristic ring pattern. This simple phenomenon is potentially important in many areas of both scientific and industrial applications [8, 9, 10, 11]. This evaporation mechanism can create very fine lines of deposition in a robust way that requires no explicit forming. Further, it is a way of concentrating material strongly in a quantitatively predictable way. Lastly, it creates capillary flow patterns that can be useful for processing of polyatomic solutes like DNA [12, 13, 14].

In the work of Popov and Witten [5, 6], the flow field and the rate of growth of the deposit patterns in a drop pinned over an angular sector on plane substrate have been studied. The fluid flow near the singularity of the vertex was calculated, and basic assumptions established. It was found that the solution in the angular region has many features which are not shared by the solution in the circular geometry obtained in [2, 3, 4]. In particular, three time regimes have been defined, where relevant physical quantities follow different scaling properties, and all the universal scaling exponents depend on the opening angle of the sector in a predictable way.

In this paper we treat this same geometry under simpler evaporation condition: the evaporation occurs *uniformly* over the liquid surface. In contrast, Refs. 3, 4 and 6 treated the more prevalent but more complicated case of diffusion-controlled evaporation, where the local evaporation rate is proportional to the local gradient of vapor concentration. This evaporation profile is singular near

the apex of the drop and is thus very nonuniform.

To understand the uniform evaporation case is conceptually important and experimentally relevant. Conceptually, we seek a fundamental understanding of how evaporation can produce singular capillary flows and singular solute deposition. Thus we seek the simplest situation in which these phenomena occur. From this point of view, the diffusion-controlled case is unnecessarily complicated. It has an extra singular feature in the evaporation profile that is not essential to the basic phenomenon. Further, the uniform evaporation case can readily be realized experimentally, following e.g. the method used in Ref. 3. It is sufficient to surround the evaporating drop under study by a large flat pool of liquid that is separated from the drop by a narrow gap. Then the vapor concentration is virtually independent of position on the surface, and the evaporating flux is uniform.

This work is to a large extent a mere application of the general theory of Ref. 6. We explore the explicit features of the uniform evaporation in the same spirit as Ref. 6 explored them for the diffusion-controlled case. As shown below, this simpler case allows a more simplified treatment, and the contrast between the two cases is both instructive and of practical interest. Moreover, we are able to avoid the uncontrolled approximations that were necessary in Ref. 6.

The paper is organized in comparison with Ref. 6. At first, we review the basic physical model and its mathematical framework, which was first introduced in Ref. 6. Next, the system is solved both analytically and numerically to reveal the physics of the model: the flow field configuration is described, and its asymptotic properties studied. We obtain the power law of the deposition rate in early time regime and intermediate time regime respectively. We then compare our results with those of diffusion-controlled case. More discussions and conclusion follow in the last sections.

*Electronic address: ruizheng@uchicago.edu

[†]Current address: Department of Physics, University of Michigan, Ann Arbor, MI 48109

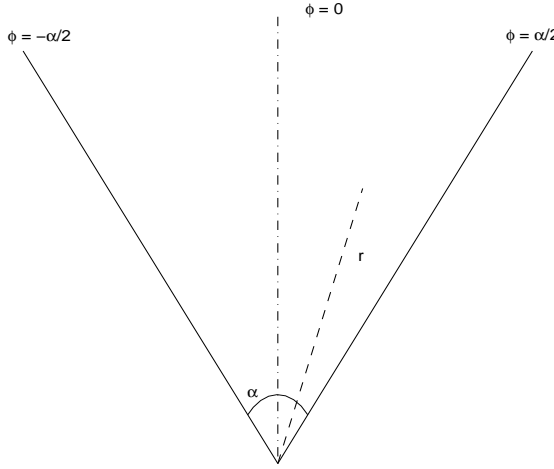


FIG. 1: Sketch of the angular drop showing geometrical quantities used in the text

II. STATEMENT OF THE PROBLEM

Following Ref. 5, we consider a droplet of solution bounded in an angular region, as shown in Fig. 1, with opening angle α on a horizontal surface of the substrate. Cylindrical coordinates (r, φ, z) are used to describe our system, with the range $0 < r < \infty$ and $-\frac{\alpha}{2} < \varphi < \frac{\alpha}{2}$, and z is the coordinate normal to the substrate.

The shape of the surface, described by the height function $h(r, \varphi, t)$, is restricted by Laplace equation:

$$\Delta p = -2H\sigma, \quad (1)$$

where Δp is the pressure difference between the fluid and atmosphere, and generally varies with local coordinates and time, σ is the surface tension, and H the mean curvature of the drop surface, which depends on h algebraically. Let \mathbf{u} be the flow velocity, and \mathbf{u}_s be its in-plane component. If we define the depth-averaged flow velocity by

$$\mathbf{v} = \frac{1}{h} \int_0^h \mathbf{u}_s dz, \quad (2)$$

we have the mass conservation equation in the form [6]:

$$\nabla \cdot (h\mathbf{v}) + \frac{J_0}{\rho} \sqrt{1 + (\nabla h)^2} + \partial_t h = 0, \quad (3)$$

where ρ is the density of the fluid, and J_0 the evaporation rate. To get the system closed, we need yet another equation, which is the Navier-Stokes equation, under the condition of low Reynolds number (that is, we drop the inertial terms in the equation):

$$\nabla p = \eta \nabla^2 \mathbf{u}, \quad (4)$$

where p is the fluid pressure, and η is the dynamic viscosity.

Further physical considerations and simplifications are needed to solve the system analytically. Firstly, as we are considering the thin drop, there is a separation of the vertical and horizontal scales in this problem, and several simplifications follow [6]. The pressure inside the drop p does not depend on the z coordinate, $\partial_z p = 0$. The surface of the drop should have a small slope, $|\nabla h| \ll 1$. And the z -derivatives of flow dominate i.e. $|\partial_z u_i| \gg |\partial_s u_i|$, where s represents any direction parallel to the substrate plane, and u_i refers to any velocity component. Under these considerations, (4) has the form [6]

$$\nabla_s p = \eta \partial_{zz} \mathbf{u}_s. \quad (5)$$

With boundary conditions: $\mathbf{u}_s|_{z=0} = 0, \partial_z \mathbf{u}_s|_{z=h} = 0$, we obtain

$$\mathbf{u}_s = \frac{\nabla p}{\eta} \left(\frac{z^2}{2} - hz \right). \quad (6)$$

With expressions (2) and (6), we have [6]

$$\mathbf{v} = -\frac{h^2}{3\eta} \nabla p. \quad (7)$$

Secondly, we are treating slow flow, and the velocity is much smaller than $v^* = \frac{\sigma}{3\eta}$, which is 24 m/s for water under normal conditions [6]. Let \tilde{v} be the characteristic velocity in this problem, which we expect to be several micrometers per second. Using standard perturbation expansion in terms of the small parameter $\epsilon = \frac{\tilde{v}}{v^*}$, let $p = p_0 + \epsilon p_1 + \epsilon^2 p_2 + \dots$, $h = h_0 + \epsilon h_1 + \epsilon^2 h_2 + \dots$, and plug them into Eqs. (1), (3) and (7), retaining only main order results, we finally have [6]

$$2H = -\frac{p_0 - p_{atm}}{\sigma}, \quad (8)$$

$$\nabla \cdot (h_0^3 \nabla \psi) = -\frac{J_0}{\rho} - \partial_t h_0, \quad (9)$$

$$\mathbf{v} = h_0^2 \nabla \psi, \quad (10)$$

where $\psi = -\frac{\epsilon p_1}{3\eta}$, and in particular, p_0 does not vary with (r, φ) , and is only a function of time t . Thus one can use (8) to determine the drop surface shape h_0 , then solve for $\psi(r, \varphi, t)$ with (9), which in turn gives the velocity field by (10). To simplify the notation, we will write $p_0 - p_{atm}$ as Δp , and h as h_0 in the rest of the paper.

Eq. (8) introduces a length scale into the problem, i.e. the mean radius of curvature $R(t) = \frac{\sigma}{\Delta p}$. It can be readily shown [6], that

$$R(t) = \frac{R_i}{1 - \frac{t}{t_f}}, \quad (11)$$

where R_i is the initial mean radius of curvature, and t_f is the total drying time. Thus in the early drying stage ($t \ll t_f$), which is the only case we are to consider in this paper, the time dependence of R can be ignored. We may generally treat $R(t)$ as constant R_i in the rest of the paper, keeping in mind its time dependence (11).

III. MATHEMATICAL EXPOSITIONS

A. Surface shape

Equation (8) under the assumption of small slope of the surface, if written explicitly in terms of $h(r, \varphi, t)$, reduces to

$$\nabla^2 h = -\frac{\Delta p}{\sigma}, \quad (12)$$

with boundary conditions $h(r, -\frac{\alpha}{2}) = h(r, \frac{\alpha}{2}) = h(0, \varphi) = 0$ [6]. As discussed in the previous section, here Δp is only a function of time, and does not depend on (r, φ) , and introduces the length scale into this equation: $R(t) = \frac{\sigma}{\Delta p}$. We are only interested in the asymptotic limit $r \ll R(t)$. This problem is quite classical [15], as for acute opening angles $0 < \alpha < \frac{\pi}{2}$, there exists a solution of the form

$$\tilde{h}(\varphi) = \frac{1}{4} \left(\frac{\cos(2\varphi)}{\cos \alpha} - 1 \right), \quad (13)$$

which is independent of remote boundary condition specifying the surface shape in the bulk of the drop. This solution diverges when α approaches the right angle from below. For $\alpha > \frac{\pi}{2}$, one has to use standard method of series expansion to find the leading order term.

The lowest order term of r in the full expansion of h in the limit $r \ll R_i$ has been found in the following form in Ref. 5:

$$h(r, \varphi, t) = \frac{r^\nu}{R(t)^{\nu-1}} \tilde{h}(\varphi), \quad (14)$$

with

$$\tilde{h}(\varphi) = \frac{1}{4} \left(\frac{\cos(2\varphi)}{\cos \alpha} - 1 \right), \quad \nu = 2 \quad 0 \leq \alpha < \frac{\pi}{2} \quad (15)$$

$$\tilde{h}(\varphi) = C(\alpha) \cos \frac{\pi \varphi}{\alpha}, \quad \nu = \frac{\pi}{\alpha} \quad \frac{\pi}{2} < \alpha \leq \pi. \quad (16)$$

The pre-factor C , which depends on α and also the remote boundary condition, has the form [5]

$$C(\alpha) = \frac{1}{4\alpha - 2\pi} + C_0 + O(\alpha - \frac{\pi}{2}), \quad (17)$$

where C_0 , which is independent of α , can be only determined by fixing the remote boundary condition. When needed in numerical simulation, we set C_0 to 1.

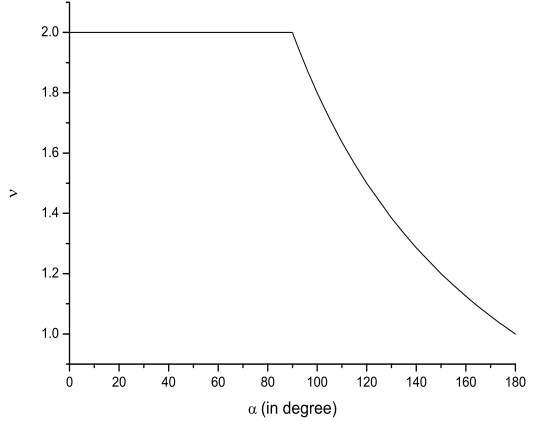


FIG. 2: Relation between the exponent ν and the opening angle α

The special case $\alpha = \frac{\pi}{2}$ invites further explanations. According to expressions (15) and (16), $\tilde{h}(\varphi)$ diverges when opening angle α approaches $\frac{\pi}{2}$ from either side. This divergence is artificial, however [6]. We will look into this issue again in Appendix B. In the rest of the paper, we will treat $\alpha = \frac{\pi}{2}$ as the limiting case, using expressions (15) and (16), keeping the possible divergence in mind.

As the exponent ν is very important in our following analysis, we show the relation between ν and the opening angle α in Fig. 2.

B. Flow field equation

Now we are ready to solve equation (9). As we are interested only in the asymptotic behavior when $r \rightarrow 0$, and $r \ll R$, from (14) we know $\partial_t h \propto r^\nu$, and compared to the constant term $\frac{J_0}{\rho}$, $\partial_t h$ can be safely dropped when we go to the asymptotic limit [6]. Physically speaking, in the asymptotic region of angular sector and in the early drying stage, the fluid mass transport due to flow flux gradient is uniquely balanced by the evaporation flux locally at each moment, with the mass change brought about by the local height change being higher order smaller quantity, and justifiably ignored.

The asymptotic solution $\psi(r, \varphi, t)$ can be expressed as:

$$\psi(r, \varphi, t) = \frac{J_0}{\rho} \frac{r^{2-3\nu}}{R(t)^{3-3\nu}} \tilde{\psi}(\varphi), \quad (18)$$

where the exponent of r is determined by simply counting the power of r on the left side of Eq. (9). From (9) and (18), we find explicitly the differential equation that $\tilde{\psi}(\varphi)$

should satisfy [6]

$$\frac{d^2\tilde{\psi}}{d\varphi^2} + \frac{3}{\tilde{h}} \frac{d\tilde{h}}{d\varphi} \frac{d\tilde{\psi}}{d\varphi} - 2(3\nu - 2)\tilde{\psi} = -\frac{1}{\tilde{h}^3}. \quad (19)$$

This equation is implicitly indexed by the opening angle, as $-\frac{\alpha}{2} \leq \varphi \leq \frac{\alpha}{2}$, ν and \tilde{h} depend on α as in (15) and (16).

The boundary conditions associated with Eq. (19) need to be clarified. Firstly, we expect the flow field to be totally symmetrical with respect to the bisector $\varphi = 0$, and therefore $\tilde{\psi}$ should be even in φ :

$$\frac{d\tilde{\psi}(0)}{d\varphi} = 0. \quad (20)$$

Secondly the outer boundary condition at $\varphi = \frac{\alpha}{2}$ amounts to the statement that no mass flows inward or outward via the contact lines. As shown in Appendix A, this amounts to the statement

$$\tilde{h}^3 \frac{d\tilde{\psi}}{d\varphi} \Big|_{\frac{\alpha}{2}} = 0. \quad (21)$$

To make the boundary condition (21) easier to handle mathematically, we define the regularized function:

$$\tilde{\chi} = \tilde{h}^2 \tilde{\psi}, \quad (22)$$

where \tilde{h}^2 is introduced to compensate for the possible second order divergence in $\tilde{\psi}$ at contact lines as shown in Appendix A. The original problem is converted to the standard boundary value problem:

$$\tilde{h} \frac{d^2\tilde{\chi}}{d\varphi^2} - \frac{d\tilde{h}}{d\varphi} \frac{d\tilde{\chi}}{d\varphi} - \left(2 \frac{d^2\tilde{h}}{d\varphi^2} + 2(3\nu - 2)\tilde{h} \right) \tilde{\chi} = -1 \quad (23)$$

$$\frac{d\tilde{\chi}}{d\varphi}(0) = 0, \quad \tilde{\chi}\left(\frac{\alpha}{2}\right) = 0,$$

where $\tilde{\chi}$ is defined in the domain $-\frac{\alpha}{2} \leq \varphi \leq \frac{\alpha}{2}$, and is even in φ .

The introduction of the regularized pressure function $\tilde{\chi}$ is universal in that it could be readily defined with more general and singular evaporation concentration. As in (22), \tilde{h} is independent of the evaporation, and its exponent 2 is determined to compensate for the singularities of the reduced pressure function $\tilde{\psi}$ in the uniform evaporation case. With a more general evaporation concentration, the singular behavior of $\tilde{\psi}$ maybe modified by singular evaporation profile, and the exponent of \tilde{h} in (22) can be adjusted accordingly. It can be shown that in the case of diffusion-controlled evaporation, the exponent becomes $\frac{5}{2}$, because of the divergence of the evaporation concentration at the contact lines.

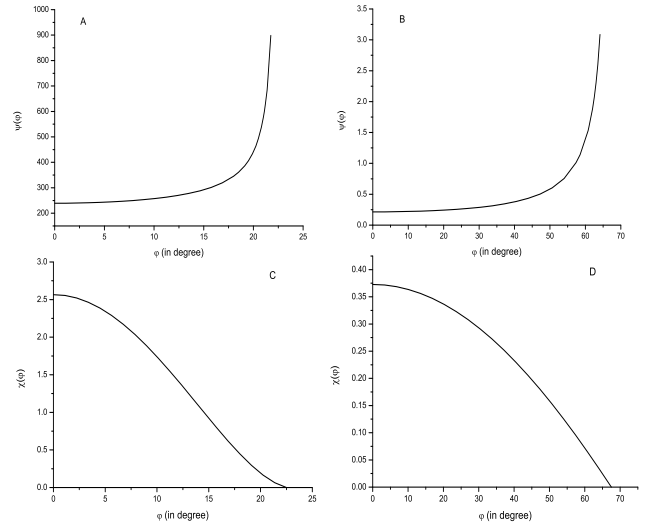


FIG. 3: A, B: The reduced pressure function $\tilde{\psi}(\varphi)$ for representative acute and obtuse opening angles. A: $\alpha = \frac{\pi}{4}$, B: $\alpha = \frac{3\pi}{4}$; C, D: The regularized function $\tilde{\chi}(\varphi)$ corresponding to A and B

We will be using both functions $\tilde{\psi}$ and $\tilde{\chi}$ in the rest of the paper. $\tilde{\chi}$ will be employed to obtain analytical as well as numerical results, because of its regularity. And $\tilde{\psi}$ will be frequently turned to in asymptotic analysis, because of its simple asymptotic form and direct connection between its singular behavior at the contact lines and the power laws of some physical properties of the system. We show the numerical solutions of $\tilde{\psi}(\varphi)$, $\tilde{\chi}(\varphi)$ for the typical opening angles $\alpha = \frac{\pi}{4}, \frac{3\pi}{4}$ in Fig. 3.

We observe that both $\tilde{\psi}(\varphi)$ and $\tilde{\chi}(\varphi)$ are much larger in the case of the typical acute opening angle $\alpha = \frac{\pi}{4}$, and slopes of $\tilde{\chi}(\varphi)$ are different when approaching $\frac{\alpha}{2}$ in these two cases. We attribute those phenomena to the qualitatively different property of the surface shape with respect to the acute and obtuse opening angles, as was previously studied in Ref. 5.

For $\frac{\pi}{2} < \alpha \leq \pi$, with result (16), Eq. (23) reduces to:

$$\cos\left(\frac{\pi\varphi}{\alpha}\right) \frac{d^2\tilde{\chi}}{d\varphi^2} + \frac{\pi}{\alpha} \sin\left(\frac{\pi\varphi}{\alpha}\right) \frac{d\tilde{\chi}}{d\varphi} + 2 \cos\left(\frac{\pi\varphi}{\alpha}\right) \left(\frac{\pi}{\alpha} - 1\right) \times \times \left(\frac{\pi}{\alpha} - 2\right) \tilde{\chi} = -\frac{1}{C(\alpha)}, \quad (24)$$

which is completely solvable for special angle π :

$$\tilde{\chi} = \frac{1}{C(\pi)} \cos \varphi, \quad \alpha = \pi. \quad (25)$$

C is α dependent according to (17), and diverges when α

approaches $\frac{\pi}{2}$ from above. If written in terms of Cartesian coordinates (we identify the x axis with the contact line, which is flat when $\alpha = \pi$, and y axis with the bisector line), with results (16), (18), (22) and (25), the reduced pressure function ψ has the form

$$\psi = \frac{J_0}{\rho} \frac{1}{C^3(\pi)} \frac{1}{y}. \quad (26)$$

We'll see later that (26) is fully consistent with the symmetry of the system when $\alpha = \pi$.

For $0 \leq \alpha < \frac{\pi}{2}$, no special angle exists to reduce the complexity of the equation. It seems that at this stage that π is the only opening angle at which we can obtain analytic results in a closed form. For $\alpha = \pi$, the speciality is well anticipated, since it is the limit case in our model: there is no apex at all. And many properties of the system associated with this case can be attributed to the symmetry of this special geometry, and revert to the simple case of a smooth, straight boundary. We will use the exact solution at the opening angle π to test our general numerical and asymptotic results.

IV. PHYSICAL PROPERTIES OF THE SYSTEM: NUMERICAL AND ANALYTIC RESULTS

A. Flow field

According to (10), if we express the velocity field in the polar coordinate system:

$$\mathbf{v} = v_r \hat{r} + v_\varphi \hat{\varphi}, \quad (27)$$

we have [6]

$$\begin{aligned} v_r &= -(3\nu - 2) \frac{J_0}{\rho} \left(\frac{r}{R(t)} \right)^{1-\nu} \tilde{h}^2 \tilde{\psi} \\ &= -(3\nu - 2) \frac{J_0}{\rho} \left(\frac{r}{R(t)} \right)^{1-\nu} \tilde{\chi}, \end{aligned} \quad (28)$$

$$\begin{aligned} v_\varphi &= \frac{J_0}{\rho} \left(\frac{r}{R(t)} \right)^{1-\nu} \tilde{h}^2 \frac{d\tilde{\psi}}{d\varphi} \\ &= \frac{J_0}{\rho} \left(\frac{r}{R(t)} \right)^{1-\nu} \left(\frac{d\tilde{\chi}}{d\varphi} - \frac{2\tilde{\chi}}{\tilde{h}} \frac{d\tilde{h}}{d\varphi} \right). \end{aligned} \quad (29)$$

As we assume that solute particles carried by the fluid moves with the same velocity as the flow itself, the trajectory of each particle can be obtained as streamlines of the flow field, which is the integration of the velocity field [6]:

$$\frac{dr}{rd\varphi} = \frac{v_r}{v_\varphi} = -(3\nu - 2) \tilde{\psi} \left(\frac{d\tilde{\psi}}{d\varphi} \right)^{-1}. \quad (30)$$

If the particle eventually arrives at the position $(r_0, \frac{\alpha}{2})$ of the boundary, the trajectory reads as [6]

$$r(\varphi) = r_0 \exp \left((3\nu - 2) \int_{\varphi}^{\frac{\alpha}{2}} \tilde{\psi} \left(\frac{d\tilde{\psi}}{d\varphi'} \right)^{-1} d\varphi' \right). \quad (31)$$

We now consider the asymptotic property of streamlines. For $\varphi \rightarrow \frac{\alpha}{2}$, v_r vanishes due to the boundary condition, while v_φ remains finite due to the asymptotic behavior of $\frac{d\tilde{\psi}}{d\varphi}$ (A11), and can be readily expressed as

$$v_\varphi \rightarrow \frac{J_0}{\rho} \left(\frac{r}{R(t)} \right)^{1-\nu} \left| \frac{d\tilde{h}}{d\varphi} \left(\frac{\alpha}{2} \right) \right|^{-1}, \quad (32)$$

or to be more explicit, with results (15) and (16),

$$\begin{aligned} v_\varphi &\rightarrow \frac{2J_0}{\rho} \left(\frac{r}{R(t)} \right)^{-1} \frac{1}{\tan \alpha} \quad 0 \leq \alpha < \frac{\pi}{2}, \\ v_\varphi &\rightarrow \frac{J_0}{\rho} \frac{\alpha}{\pi C(\alpha)} \left(\frac{r}{R(t)} \right)^{1-\frac{\pi}{\alpha}} \quad \frac{\pi}{2} < \alpha \leq \pi. \end{aligned} \quad (33)$$

In particular, v_φ seemingly vanishes as $\alpha \rightarrow \frac{\pi}{2}$. There are some subtleties here, however. We will revisit this point in Appendix B. Consequently, as $\varphi \rightarrow \frac{\alpha}{2}$, $\frac{dr}{d\varphi} \rightarrow 0$, streamlines are perpendicular to the contact lines.

For $\varphi \rightarrow 0$, as the streamlines reach far into the bulk of the drop, we expect $r(\varphi)$ to be divergent, and its behavior depends on the asymptotic properties of $\tilde{\psi}$ or $\tilde{\chi}$, when approaching the bisector. According to Eq. (19) and boundary condition (20), the asymptotic form of ψ near the bisector is

$$\tilde{\psi} \rightarrow \tilde{\psi}(0) + \frac{1}{2} \left(2(3\nu - 2)\tilde{\psi}(0) - \frac{1}{\tilde{h}^3(0)} \right) \varphi^2. \quad (34)$$

The boundary value $\tilde{\psi}(0)$ requires the complete solution of Eq. (19). The divergent part of the integration in (31) is then uniquely determined by the asymptotic form (34) as (Eq. (50) in Ref. 6):

$$\int_{\varphi}^{\frac{\alpha}{2}} \tilde{\psi} \left(\frac{d\tilde{\psi}}{d\varphi'} \right)^{-1} d\varphi' \rightarrow \frac{1}{2(3\nu - 2) - \kappa^2} \ln \frac{\alpha}{2\varphi}, \quad (35)$$

where

$$\kappa^2 = \frac{1}{\tilde{h}^3(0)\tilde{\psi}(0)}. \quad (36)$$

And therefore the streamlines in this limit go as

$$r \rightarrow r_0 \left(\frac{\alpha}{2\varphi} \right)^\epsilon, \quad \varphi \rightarrow 0, \quad (37)$$

with

$$\epsilon = \frac{3\nu - 2}{2(3\nu - 2) - \kappa^2}. \quad (38)$$

We do not have exact analytic results for exponents $\kappa^2(\alpha)$ and $\epsilon(\alpha)$ for arbitrary opening angle α , as equations (19) and (23) can not be solved in closed form to obtain $\tilde{\psi}(0)$. For special opening angle π , it is straightforward to solve for the streamline equation and velocity components, via (25):

$$r \sin \varphi = r_0, \quad (39)$$

$$v_r = -\frac{J_0}{\rho} \frac{\cos \varphi}{C(\pi)}, \quad v_\varphi = \frac{J_0}{\rho} \frac{\sin \varphi}{C(\pi)}, \quad (40)$$

and accordingly

$$\kappa^2(\pi) = 1, \quad (41)$$

$$\epsilon(\pi) = 1. \quad (42)$$

In terms of Cartesian coordinates, (39) and (40) reduce to simple forms

$$x = r_0, \quad (43)$$

$$v_y = -\frac{J_0}{\rho} \frac{1}{C(\pi)}. \quad (44)$$

The streamline configuration (43) and velocity (44) in the case of $\alpha = \pi$ are fully consistent with the symmetry of the system, since the position of the apex is no longer well defined when $\alpha = \pi$.

For arbitrary opening angle α , we solve the boundary value problem (23) numerically to fix $\tilde{\chi}(0)$ (so as to fix $\tilde{\psi}(0)$), and determine the dependence of κ^2 , ϵ on the opening angle α , as shown in Fig. 4 and Fig. 5, which are in agreement with analytic results (41) and (42).

The exponent ϵ determines geometrically the asymptotic behavior of streamlines near the bisector $\varphi = 0$. According to (37), the distance between the streamline and the bisector scales with φ as $\varphi r(\varphi) \propto \varphi^{1-\epsilon}$ when φ approaches 0. From Fig. 5, we know that for $\alpha = \frac{\pi}{2}$, π , $\epsilon = 1$, hence $\varphi r(\varphi)$ remains constant asymptotically. Geometrically, this means that streamlines run parallel to the bisector, when $\varphi \rightarrow 0$. This result also follows straightforwardly from our analytic solution (39). For $\alpha = \pi$, this geometric property of streamlines is well anticipated considering the symmetry of the system, for $\alpha = \frac{\pi}{2}$, however, it is quite subtle. For acute opening angles, we find out $\epsilon < 1$, and therefore the asymptotic distance decreases when $\varphi \rightarrow 0$, and the streamlines are converging toward the bisector as $r \rightarrow \infty$. The incoming particles, in this case, are moving along the trajectory away from the bisector. For obtuse opening angles, we have $\epsilon > 1$, and therefore the asymptotic distance increases when $\varphi \rightarrow 0$, and the streamlines are diverging away from the bisector as $r \rightarrow \infty$. The incoming particles,

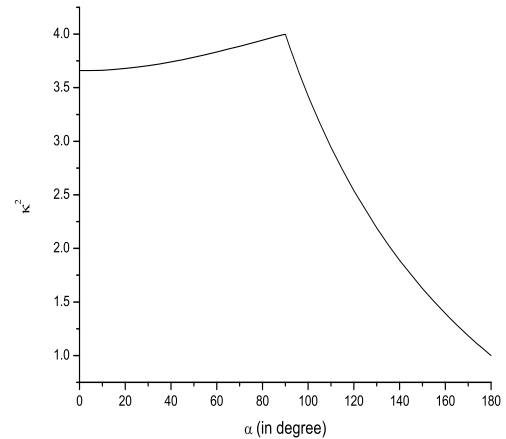


FIG. 4: Dependence of parameter κ^2 on opening angle α

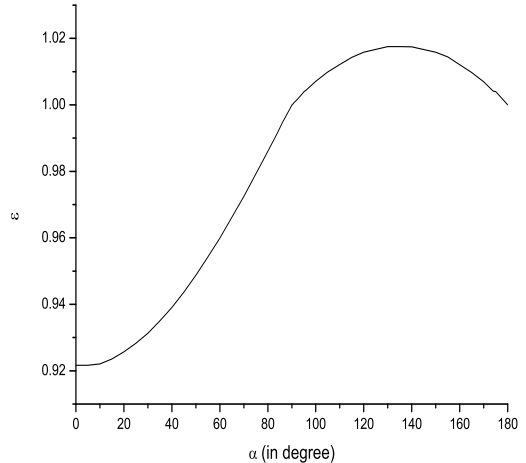


FIG. 5: Dependence of the stream line asymptotic exponent ϵ (when $\varphi \rightarrow 0$) on the opening angle α

in this case, first move along the trajectory toward the bisector, reaches a minimum distance, and then turn away toward the contact lines. In diffusion-controlled flow [6], this behavior was found for all opening angles. In Fig. 6, we show the flow field configuration for the opening angle $\alpha = \frac{\pi}{2}$.

These flow trajectories are independent of dimensional quantities like the evaporation rate J , and they depend only on the opening angle [6]. Hence the trajectory of the moving solute particle does not depend on how fast the drop evaporates and how thin the liquid layer is.

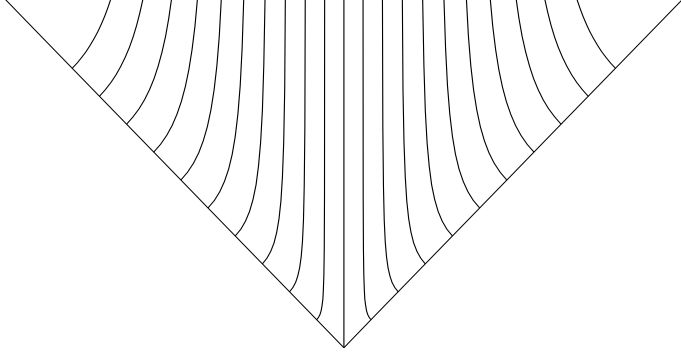


FIG. 6: Streamline configuration for the opening angle $\frac{\alpha}{2}$

B. Solute transfer and deposit growth

As in the diffusion-controlled case (Eqs. (55) and (56) in Ref. 6), one can now calculate the time it takes for the solute particle initially located at (r, φ) (due to the symmetry of the system, we assume $\varphi \geq 0$) to move along the streamline to the contact line $(r_0, \frac{\alpha}{2})$. We reproduce the results below:

$$t = \int_{\varphi}^{\frac{\alpha}{2}} \frac{rd\varphi'}{v_{\varphi}} = t_0 \int_{\varphi}^{\frac{\alpha}{2}} \frac{\exp \left(\nu (3\nu - 2) \int_{\zeta}^{\frac{\alpha}{2}} \tilde{\psi}(\xi) \left(\frac{d\tilde{\psi}}{d\xi} \right)^{-1} d\xi \right)}{\tilde{h}^2 \frac{d\tilde{\psi}}{d\xi}} d\zeta, \quad (45)$$

where

$$t_0 = \frac{\rho}{J_0} \frac{r_0^{\nu}}{R(t)^{\nu-1}} \rightarrow \frac{\rho}{J_0} \frac{r_0^{\nu}}{R_i^{\nu-1}}, \quad (46)$$

is the combination of prefactors, and has a dimension of time. In the early stage of the drying process, we can approximate $R(t)$ by R_i , and t_0 is therefore independent of t .

For each position on the contact line indexed by r_0 , and for each time t , there exists a unique $\varphi(r_0, t)$ de-

termined by Eq. (45), and all the solute located in the area bounded by neighboring streamlines indexed by r_0 , $r_0 + dr_0$, in the domain $\varphi(r_0, t) \leq \zeta \leq \frac{\alpha}{2}$, will have reached the contact line and become part of the deposit within time t . If we assume that initially at $t = 0$ the solute has constant concentration c_0 everywhere in the drop, then the amount of mass deposit can be expressed as (Eq. (58) in Ref. 6):

$$dm(r_0, \varphi) = c_0 \frac{r_0^{\nu+1}}{R_i^{\nu-1}} dr_0 \int_{\varphi}^{\frac{\alpha}{2}} \tilde{h}(\zeta) \exp \left((\nu + 2)(3\nu - 2) \int_{\zeta}^{\frac{\alpha}{2}} \tilde{\psi}(\xi) \left(\frac{d\tilde{\psi}}{d\xi} \right)^{-1} d\xi \right) d\zeta. \quad (47)$$

Using the same method as in Ref. 6, one can solve for $\varphi(t)$ from (45), and plug it into (47) to obtain the deposition rate $\frac{dm(r_0, t)}{dr_0}$.

Again, we can start with special opening angle π , for which analytic results can be obtained. With (25), (45), (47), we have for $\alpha = \pi$

$$t(\varphi) = C(\pi) t_0 \cot \varphi, \quad t_0 = \frac{\rho}{J_0} r_0, \quad (48)$$

$$\frac{dm}{dr_0}(r_0, \varphi) = c_0 C(\pi) r_0^2 \frac{1}{2} \left(\frac{1}{\sin^2 \varphi} - 1 \right). \quad (49)$$

And the power law reads as

$$\frac{dm}{dr_0} = \frac{c_0}{C(\pi)} \frac{1}{2} \left(\frac{J_0}{\rho} \right)^2 t^2. \quad (50)$$

The deposition rate for $\alpha = \pi$ does not depend on r_0 , which is anticipated, since the position of the apex is no longer well defined. The exact result (50) can also be obtained with the surface shape (16) and velocity (44). For the special case of $\alpha = \pi$, in Cartesian coordinates, we have

$$h = C(\pi)y, \quad (51)$$

$$v_y = -\frac{J_0}{\rho} C(\pi), \quad (52)$$

$$y = v_y t, \quad (53)$$

And

$$\frac{dm}{dr_0}(t) = \frac{1}{2} c_0 v_y t h(t). \quad (54)$$

Result (50) follows immediately.

For $\alpha = \pi$, there is a unique power law (50) in the whole domain of φ and for all time t in the early drying stage. For arbitrary opening angles α other than π , however, those integrations in (45) and (47) can not be calculated explicitly, without knowledge of the closed form of $\tilde{\psi}(\varphi)$. Instead, we have to analyze (45) and (47) asymptotically in two different limiting cases: $\varphi \rightarrow 0$ and $\varphi \rightarrow \frac{\alpha}{2}$. In the framework of the physical system, these two different asymptotic regions correspond to two different time regimes, when the deposition rate follows different power laws, as first introduced in Ref. 6:

early time regime: $t \ll t_0$, when only solute particles initially located near to the boundary can reach the contact line and become part of the deposit. Properties of deposition in the time regime are governed by the mathematical asymptotic $\varphi \rightarrow \frac{\alpha}{2}$.

intermediate time regime: $t_0 \ll t \ll t_f$, when solute particles initially located near to the bisector can reach the contact line. And in this time regime we consider in the limit $\varphi \rightarrow 0$. The condition $t \ll t_f$, where t_f is the total drying time, means that we are considering the early drying stage, where the theory applies.

As argued in Ref. 6, the separation of two time regimes works worse when the opening angle α increases towards π . This can be readily seen in our case, as shown in (50), when $\alpha = \pi$, the deposition rate follows the same power law throughout the early drying stage, and the two time regimes are not distinguishable.

1. Deposit growth in the early time regime

In the early time regime, the mass deposition is contributed by the solute particles initially located near the contact lines. Using expressions (45) and (47) in the limit $\varphi \rightarrow \frac{\alpha}{2}$, as well as the expression for t_0 (46), which contains a factor of r_0^ν , we find the power law of the deposition rate (compared to Eq. (60) in Ref. 6):

$$\frac{dm}{dr_0}(r_0, t) \propto t^2 r_0^\beta, \quad (55)$$

with

$$\beta(\alpha) = 1 - \nu, \quad (56)$$

which is in agreement with the results we've obtained previously for special angle π (50).

The relation (56) is understandable in the following way. As argued before, let δ be the distance from the contact line. When δ is small, mass conservation demands $h\mathbf{v} \propto J\delta$, hence $\mathbf{v} \propto (\frac{dh}{d\delta})^{-1}$, that is, near contact lines the velocity should be inversely proportional to the slope of the drop surface i.e. $|\frac{\partial h}{\partial \delta}|$. According to (14), near the contact line $h = r^\nu \tilde{h}(\varphi) \approx r^\nu \tilde{h}(\frac{\alpha}{2} - \frac{\delta}{r})$, and $|\frac{\partial h}{\partial \delta}| \propto r^{\nu-1} \frac{d\tilde{h}}{d\varphi} \Big|_{\frac{\alpha}{2}}$. Hence the velocity is proportional to $r^{1-\nu}$, so is the mass deposition rate, and (56) follows.

2. Deposit growth in the intermediate time regime

In the intermediate time regime, we consider in the limit $\varphi \rightarrow 0$. In this limit, we can use expressions (34), (35) to obtain the asymptotic forms of (45) and (47), and we find the deposition rate to be (compared to Eq. (63) in Ref. 6):

$$\frac{dm}{dr_0}(r_0, t) \propto t^\delta r_0^\gamma, \quad (57)$$

with scaling exponents:

$$\delta = 1 + \frac{\kappa^2}{\nu(3\nu - 2)}, \quad (58)$$

$$\gamma = 1 - \frac{\kappa^2}{3\nu - 2}. \quad (59)$$

Again (58) and (59) are in agreement with the values of scaling exponents we've obtained for special angle π . Using our previous numerical result for κ^2 (Fig. 4), we show the dependence of exponents δ and γ on the opening angle α in Fig. 7, Fig. 8.

V. COMPARISON WITH DIFFUSION-CONTROLLED EVAPORATION

Popov and Witten [6] considered a general evaporation profile $J(r, \varphi)$ of the limiting form

$$J \rightarrow r^{\mu-1} (\frac{\alpha}{2} - |\varphi|)^{-\lambda}, \quad |\varphi| \rightarrow \frac{\alpha}{2}. \quad (60)$$

The uniform case treated here corresponds to $\mu = 1$, $\lambda = 0$. The results of the previous section may be obtained by setting $\mu = 1$, $\lambda = 0$ in the general expressions of Ref. 6. In some cases this limit permits simpler expressions and more explicit solutions as we have seen. For the diffusion-controlled case $\lambda = \frac{1}{2}$ and μ is an explicit function of the opening angle α as shown in Fig. 9, reflecting the singular behavior of the Laplacian vapor concentration field. We now summarize the difference in the two asymptotic regimes of interest.

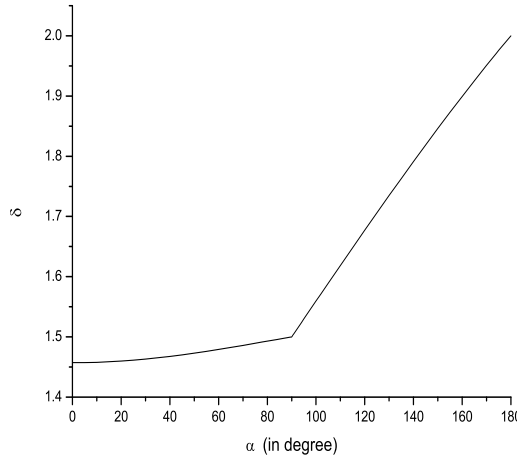


FIG. 7: Relation between the exponent δ of the deposit time t in the intermediate time regime and the opening angle α , in the asymptotic scaling of the deposit rate

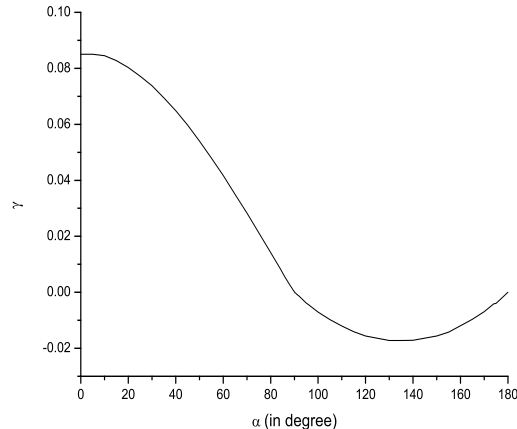


FIG. 8: Relation between the exponent γ of the contact line distance r_0 in the intermediate time regime and the opening angle α , in the asymptotic scaling of the deposit rate

A. Near contact line physics

In this case, only the asymptotic form of the evaporation J as in (60) when φ approaches $\pm\frac{\alpha}{2}$ matters. While μ is relevant to the dependence of the reduced pressure function ψ on coordinate r , the exponent λ governs the singular property of the reduced pressure function near contact lines (a direct observation is that, due to none zero value of $\lambda = \frac{1}{2}$ in the diffusion-controlled evaporation, the order of divergence of $\tilde{\psi}$ is higher by $\frac{1}{2}$ in that case). For near contact line physics, or the deposition rate in the early time regime, the power law found in the diffusion-controlled evaporation case [6], as well as our

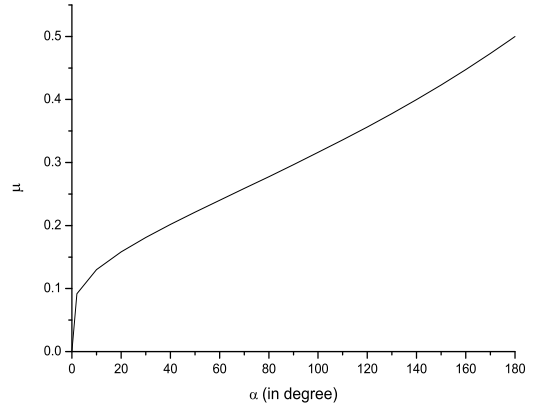


FIG. 9: Relation between the exponent μ and the opening angle α , in the case of diffusion-controlled evaporation from an angular region

result (55), obtained as a reduced case by setting $\mu \equiv 1$, $\lambda \equiv 0$, is uniquely determined by the local singular property of the reduced pressure function at contact lines, and those power law exponents have simple algebraic expressions in terms of μ , λ and ν .

Both Ref. 6 and our result show that the exponent of time t in the power law of deposition rate remains independent of the opening angle α in the early time regime, though in our case the deposition process goes slower with exponent 2, instead of $\frac{4}{3}$ in Ref. 6. As regard to the dependence on the contact line distance r_0 , both Ref. 6 and our result (56) show that β always remains between -1 and 0 for obtuse opening angle α , and the integrability of the singularity at $r_0 = 0$ holds. As argued in Ref. 6, this states that although the deposition rate is larger there, the vertex of the sector does not dominate the sides and that the deposition accumulation at the vertex is not qualitatively different from the deposition accumulation on the sides for obtuse opening angles.

For acute opening angle α , although β remains between -1 and 0 in Ref. 6, it is constantly -1 in our case. It seems that we've got a more concentrated deposition pattern with a nonsingular form of evaporation rate. The singular flow of the diffusion-controlled evaporation J in Ref. 6 presumably deflects the streamlines towards the contact lines more than in our case, and hence drives more fluid and mass to the sides and thus away from the apex.

Furthermore, the $\frac{1}{r_0}$ dependence of the deposition rate we've obtained in the early time regime for acute opening angle α seems to violate the integrability, and suggest a logarithmic divergence: an arbitrarily large fraction of the mass may occur for an arbitrarily small distance. To resolve this possible singularity, a cutoff has to be introduced, which is naturally related with the definition of

the time scale t_0 (46)

$$t_0 = \frac{\rho}{J_0} \frac{r_0^\nu}{R_i^{\nu-1}}. \quad (61)$$

Accordingly, for each time t , one can define the crossover length

$$r^*(t) = \left(t R_i^{\nu-1} \frac{J_0}{\rho} \right)^{\frac{1}{\nu}}. \quad (62)$$

For the early time regime we have $t \ll t_0$, and therefore for each time t , only the region $r_0 \gg r^*(t)$ on contact lines is in the early time regime with respect to the time t , and the very smallest r_0 's are always in the intermediate time regime. The cutoff $r^*(t)$ actually saves the mass deposition from being logarithmically infinite.

B. Near bisector line physics

Physics in this category (the configuration of the streamlines near the bisector, deposition rate in the intermediate time regime) is related to the limit $\varphi \rightarrow 0$. An important parameter which dominates the physics in this category is the boundary value of the reduced pressure function at the bisector: $\tilde{\psi}(0)$, or the parameter κ^2 . Near the bisector both the evaporation concentration J and function $\tilde{\psi}$ are regular, and both $\tilde{\psi}(0)$ and κ^2 depend on the whole differential structure of the main equation (19), in the full range of domain of φ , from 0 to $\frac{\alpha}{2}$, as well as the possible singular behavior of J at contact lines.

The most interesting result in this category is certainly the qualitatively different behaviors of physical quantities in acute opening angle geometry versus in obtuse opening angle geometry. Abrupt changes take place at the right opening angle of the sector $\alpha = \frac{\pi}{2}$, as compared to Ref. 6. Our numerical result for κ^2 (Fig. 4) is not qualitatively different from that obtained in Ref. 6, as κ^2 changes dramatically at $\alpha = \frac{\pi}{2}$ in both cases. This is understandable, because the non-smoothness at $\alpha = \frac{\pi}{2}$ is uniquely due to the crossover of the exponent ν in the leading order term determining the surface shape (results (15) and (16)), while the evaporation rate J behaves smoothly at $\alpha = \frac{\pi}{2}$ in both cases.

The flow field configuration near the bisector as $\varphi \rightarrow 0$, is governed by

$$\varphi r(\varphi) \propto \varphi^{1-\epsilon}. \quad (63)$$

In Ref. 6, $\epsilon(\alpha)$ was monotonically decreasing smoothly with α , and $\epsilon = 1$ at $\alpha = \pi$. The uniform evaporation case (Fig. 5) is dramatically different: for acute opening angle α , $\epsilon(\alpha)$ is strictly less than 1, it is strictly larger than 1 in the obtuse angle region, and a clear break in slope happens at $\alpha = \frac{\pi}{2}$, where $\epsilon = 1$.

Geometrically, in Ref. 6 where ϵ is larger than 1, except for $\alpha = \pi$, streamlines asymptotically diverge from

the bisector. In contrast, our results show that, for acute opening angles, the streamlines asymptotically converge to the bisector; while for obtuse opening angles, they diverge, and particularly for the critical angle $\frac{\pi}{2}$, streamlines run parallel to the bisector line, which is not anticipated intuitively.

As regard to the power law of the deposition rate in the intermediate time regime, we consider the asymptotic form:

$$\frac{dm}{dr_0}(r_0, t) \propto t^\delta r_0^\gamma \quad \varphi \rightarrow 0, \quad (64)$$

the result we've obtained for the exponent $\delta(\alpha)$ (Fig. 7) follows the same qualitative pattern as in Ref. 6, though is everywhere larger, so that the deposition process goes slower, as in the early time regime.

In Ref. 6, $\gamma(\alpha)$ remains negative, monotonically increases with α smoothly, and becomes 0 at $\alpha = \pi$ (compatible with the symmetry). In the uniform evaporation case, $\gamma(\alpha)$ follows a richer pattern and changes slope abruptly at $\alpha = \frac{\pi}{2}$. Physically, as γ is strictly larger than -1 , the integrability property holds. However, while γ is negative for obtuse opening angles, it becomes positive for acute angles, and therefore the deposition accumulation is in favor of the sides, rather than the vertex as shown in Ref. 6. In particular, as γ goes to 0 at $\alpha = \frac{\pi}{2}$ and its absolute value remains small nearby, it seems that the uniform evaporation case yields a relatively uniform deposition pattern for a wide range of opening angles in the intermediate time regime.

The exponent γ controlling mass deposition is closely related to the trajectory exponent ϵ . From expressions (38) and (59), we have a simple relation:

$$\epsilon = \frac{1}{1 + \gamma}, \quad (65)$$

which is also implicit in Ref. 6, though it was not discussed there. Intuitively, in the intermediate time regime, virtually all the solute between the bisector and the contact line is swept into the contact lines and becomes part of the deposit, and therefore γ , the exponent of the contact line distance r_0 which indexes streamlines, should be related to the geometric distribution of the streamlines near the bisector away from the vertex. For $\alpha = \pi$, $\frac{\pi}{2}$, $\epsilon = 1$, the streamlines are uniformly distributed near the bisector away from the vertex, and the solute is therefore uniformly carried to the contact lines by the flow, and the deposition rate should be independent of the contact line distance: $\gamma = 0$. For other angles, the streamlines become unevenly distributed away from the vertex. When $\epsilon > 1$, they diverge away from the bisector as $\varphi \rightarrow 0$, the smaller contact line distance r_0 that indexes the streamline is, the nearer the corresponding streamline to the bisector, and more solute will be carried to the spot along the streamline, and therefore the deposition is in favor of the vertex, and γ is negative. When $\epsilon < 1$, γ is positive by the same argument.

To be more precise mathematically, in the intermediate time regime $t_0 \ll t$, and in the limit $\varphi \rightarrow 0$, the deposition rate is actually independent of drop surface shape and velocity (in contrast to the early time regime, where the deposition rate is closely related to the slope of the surface shape at contact line as discussed previously), and is uniquely determined by the streamline configuration near the bisector line: the amount of solute deposited near r_0 is decided by the width of the interval between adjacent streamlines indexed by r_0 and $r_0 + \Delta r_0$ near the bisector line, which is proportional to $r \Delta \varphi$ in the limit $\varphi \rightarrow 0$. Near the bisector line, the streamline indexed by r_0 can be expressed as

$$r \propto r_0 \varphi^{-\epsilon}. \quad (66)$$

If we consider a small patch $r = \text{const.}$ near the bisector line, and study the intersections of streamlines with this patch, with (66) we have

$$0 = dr \propto \varphi^{-\epsilon} dr_0 - \epsilon r_0 \varphi^{-\epsilon-1} d\varphi, \quad (67)$$

and therefore

$$\frac{d\varphi}{dr_0} = \frac{\varphi}{\epsilon r_0}. \quad (68)$$

According to the above argument, with (66) and (68), we have

$$\frac{dm}{dr_0} \propto \frac{d\varphi}{dr_0} \propto \frac{1}{\epsilon} r_0^{\frac{1}{\epsilon}-1}, \quad (69)$$

and the relation (65) follows immediately.

VI. DISCUSSION

The theoretical framework, first established in Ref. 6 and studied here in continuation, though it captures the essential mechanism of the deposit growth, does not take into account a number of additional effects that can certainly modify the deposition, and some restrictions and shortcomings remain [6].

The crossover at the opening angle $\alpha = \frac{\pi}{2}$ (as manifested in the surface shape h (14), (15) and (16)), which is certainly independent of the evaporation concentration, is quite a subtle point of the theory. As shown in the Appendix B, in principle, modifications to the results obtained in this paper as well as in Ref. 6 via asymptotic analysis are needed in the neighborhood of the right opening angle $[\frac{\pi}{2} - \Delta\alpha, \frac{\pi}{2} + \Delta\alpha]$, with $\Delta\alpha \approx \left| \ln \frac{r}{R_i} \right|^{-1}$ (B5). The thinner and flatter the drop is, and closer to the apex i.e. $r \ll R_i$, the better our results apply.

Further, we believe that results for those relevant power law exponents obtained via asymptotic analysis are exact, except for a possible logarithmic modification at $\alpha = \frac{\pi}{2}$, where a crossover of the exponent could happen. For other experimentally testable physical quantities discussed in this paper (the velocity components,

the reduced pressure function $\tilde{\psi}$), exact properties in the neighborhood $[\frac{\pi}{2} - \Delta\alpha, \frac{\pi}{2} + \Delta\alpha]$ could be in principle interpolated, as shown in the Appendix B, as all the physical properties of the system should depend on the opening angle α continuously.

Another interesting observation is the form of evaporation rate. In this paper, we've considered uniform evaporation, which is simpler than the diffusion-controlled evaporation employed in Ref. 6. The form of evaporation is not arbitrary, and besides other physical restrictions, it should be compatible with the symmetry of the system. One such consideration would be that: in the limit $\alpha \rightarrow \pi$, the position of the apex is no longer well defined, and the deposit rate should not depend on the contact line distance r_0 , and therefore $\beta(\pi) = 0$, $\gamma(\pi) = 0$. Combined with the expression for β in the case of diffusion-controlled evaporation (Eq. 61 in Ref. 6), this condition demands

$$\lambda(\pi) + \mu(\pi) = 1. \quad (70)$$

which is satisfied in both cases (in Ref. 6, $\lambda \equiv \frac{1}{2}$, $\mu(\pi) = \frac{1}{2}$; in this paper, $\lambda \equiv 0$, $\mu \equiv 1$). In reflection, condition (70) can be explained in an explicit way: in the limit $\alpha \rightarrow \pi$, the evaporation rate should only depend on the distance from the contact line i.e. $r \sin(\frac{\alpha}{2} - |\varphi|)$, which reduces to $r(\frac{\alpha}{2} - |\varphi|)$ near the contact line as $|\varphi| \rightarrow \frac{\alpha}{2}$, and in connection with expression (60), the requirement (70) follows. For exponent γ , both our result and that of Ref. 6 give $\gamma(\pi) = 0$, but no simple relation as (70) can be obtained, since γ is related to the parameter κ^2 , which depends on the whole differential structure of the main equation (19), and the symmetry of system, which is included implicitly in this equation, needs better understanding in this case.

Theoretically, for the intermediate time regime, where, physics depends on the mathematical structure over the whole domain of φ , more thorough and analytical treatment of the main equation (19) is certainly appealing. The criticality of the opening angle $\alpha = \frac{\pi}{2}$ demands extra attention: why some physical properties divide between acute angle and obtuse angle, and why this separation did not appear in Ref. 6, where the same h entered, and how this separation is related to the form of evaporation concentration? Naively, these questions can be readily addressed by saying that the criticality of the right angle is uniquely due to the crossover of the leading terms in the full expansion of the surface shape h by solving Laplace equation or diffusion type equation in an angular region with opening angle $\alpha = \frac{\pi}{2}$. The uniform evaporation profile, without introducing further singularity, helps to retain the trace of this criticality in the resulted physical quantities and phenomena, rather than overshadowing it as in the case of diffusion-controlled evaporation. More mathematically rigorous treatment needs to be done to make this argument clearer.

Experimentally, it is interesting to note some possible applications of our results. Our work shows that uniform evaporation at early times with acute opening an-

gle achieves the greatest concentration towards the apex. Accordingly, one could actually achieve a great concentration of mass by allowing the evaporation to occur for a short time, then allowing the dissolved solute to diffuse and equilibrate, then allowing another bit of evaporation, and so forth. In this way, one could approach the behavior of having a finite fraction of the mass within some small distance of the apex. Another interesting aspect is the nearly perfect uniformity of the deposition for late time regime with opening angle $\alpha \simeq \frac{\pi}{2}$. This kind of uniform deposition may be useful, especially when a small amount of the concentrated substance is sufficient. For example, a dilute solution of reagents can be concentrated strongly at the contact line, thereby inducing a chemical reaction there. The evaporation mechanism assures that the concentration is a known function of the position and the initial dilution. Likewise, trace amounts of solute can be rendered more easily detectable by causing them to concentrate at a contact line.

VII. CONCLUSION

The uniform evaporation of an angular drop yields surprisingly rich and potentially useful behavior. This behavior complements the previously studied work on diffusion-controlled evaporation [6]. Though our case lacks the distinctive singular evaporation of the diffusion-controlled case, remarkably, it leads to a *stronger* focusing of solute towards the apex. Further, it can create two qualitatively different type of flow, according to whether the opening angle is acute or obtuse. The deposition profile is remarkably uniform for late times when the opening angle is close to a right angle. Now that these deposition properties have been established, they may well prove useful. For example, they provide a means of concentrating trace solutes in a liquid in a rapid and quantitatively predictable way. They also create distinctive capillary flow fields and distinctive concentration profiles of solute. We expect this kind of microscopic, singular, evaporative flow to play an increasing role in the technology of small scale material synthesis, processing and analysis.

Acknowledgments

This work was supported in part by the National Science Foundation's MRSEC Program under Award Number DMR-0213745.

APPENDIX A: OUTER BOUNDARY CONDITION FOR THE FLOW EQUATION

In this appendix we provide a justification of the outer boundary condition (21). In Ref. 6, Eq. (19) was solved without explicitly using a boundary condition. Instead,

Ref. 6 used the global mass conservation condition

$$\rho \int_{-\frac{\alpha}{2}}^{\frac{\alpha}{2}} |v_r| h r d\varphi = \int_0^r \int_{-\frac{\alpha}{2}}^{\frac{\alpha}{2}} J_0 r dr d\varphi, \quad (\text{A1})$$

where $v_r = h^2 \partial_r \psi$ is the flow velocity component along the direction of radius [6]. However, Eq. (19) is itself an expression of local mass conservation. Thus it is unclear why (A1) represents new information that can further restrict the solution. Here we explain the origin of the new information. We show that it takes the form of a boundary condition. And we also show that this boundary condition is sufficient to give a unique solution for $\tilde{\psi}(\varphi)$.

With the expressions of h and ψ , (A1) is simplified as:

$$\int_0^{\frac{\alpha}{2}} \left(2(3\nu - 2) \tilde{h}^3 \tilde{\psi} - 1 \right) d\varphi = 0. \quad (\text{A2})$$

The local mass conservation implicitly stated in (19) allows us to express $\tilde{\psi}$ in terms of derivative $\frac{d\tilde{\psi}}{d\varphi}$: $2(3\nu - 2)\tilde{\psi}\tilde{h}^3 = \frac{d^2\tilde{\psi}}{d\varphi^2}\tilde{h}^3 + 3\tilde{h}^2 \frac{d\tilde{h}}{d\varphi} \frac{d\tilde{\psi}}{d\varphi} + 1$. Then an integration by parts, together with the boundary condition (20), converts the integral condition (A2) into a boundary condition:

$$\tilde{h}^3 \left. \frac{d\tilde{\psi}}{d\varphi} \right|_{\frac{\alpha}{2}} = 0. \quad (\text{A3})$$

We must now show that condition (A3) does in fact restrict the general form of $\tilde{\psi}$ and leads to a unique solution. To see this, we need to study the asymptotic behavior of $\tilde{\psi}$. As both \tilde{h} and $\tilde{\psi}$ are even in φ , we only need to study in the domain $0 \leq \varphi \leq \frac{\alpha}{2}$. Let's consider the limit $\varphi \rightarrow \frac{\alpha}{2}$, and keep in mind that $\tilde{h} \propto (\frac{\alpha}{2} - \varphi)$ in this limit. From the expressions of \tilde{h} (15) and (16), as well as Eq. (19), we see that $\tilde{\psi}$ necessarily diverges in this limit, and the third term on the left side of Eq. (19), which is of the lowest order of divergence, can be neglected in the asymptotic analysis. Eq. (19) thus reduces to:

$$\frac{d^2\tilde{\psi}}{d\varphi^2} + \frac{3}{\tilde{h}} \frac{d\tilde{h}}{d\varphi} \frac{d\tilde{\psi}}{d\varphi} + \frac{1}{\tilde{h}^3} = 0. \quad (\text{A4})$$

Eq. (A4) can be solved analytically. First, consider the homogeneous first order differential equation of $\frac{d\tilde{\psi}}{d\varphi}$:

$$\frac{d}{d\varphi} \left(\frac{d\tilde{\psi}}{d\varphi} \right) + \frac{3}{\tilde{h}} \frac{d\tilde{h}}{d\varphi} \frac{d\tilde{\psi}}{d\varphi} = 0, \quad (\text{A5})$$

which has the general solution of the form:

$$\frac{d\tilde{\psi}}{d\varphi} = c \frac{1}{\tilde{h}^3}, \quad (\text{A6})$$

c being an arbitrary constant. To obtain the general solution of the inhomogeneous equation (A4), we let c be a function of φ , i.e. $\frac{d\tilde{\psi}}{d\varphi} = c(\varphi) \frac{1}{h^3}$, then plug it into (A4), and find out:

$$\frac{dc}{d\varphi} = -1, \quad (A7)$$

which shows

$$c(\varphi) = -\varphi + \tilde{c}. \quad (A8)$$

Combining (A6) and (A8), we find that Eq. (A4) (and hence Eq. (19)) has a general solution of the form:

$$\tilde{\psi} \rightarrow C_1 + C_2 \int_0^\varphi \frac{d\xi}{h^3(\xi)} - \int_0^\varphi \frac{\xi}{h^3(\xi)} d\xi, \quad \varphi \rightarrow \frac{\alpha}{2}, \quad (A9)$$

where C_1 and C_2 are arbitrary constants. We can show the divergence of $\tilde{\psi}$ in this limit more explicitly by expanding the right side of (A9) in terms of $(\frac{\alpha}{2} - \varphi)$,

$$\begin{aligned} \tilde{\psi} \rightarrow & \frac{1}{2} \left(\frac{\alpha}{2} - C_2 \right) \left(\frac{d\tilde{h}}{d\varphi} \Big|_{\frac{\alpha}{2}} \right)^{-3} \left(\frac{\alpha}{2} - \varphi \right)^{-2} \\ & - \left(\frac{d\tilde{h}}{d\varphi} \Big|_{\frac{\alpha}{2}} \right)^{-3} \left(\frac{\alpha}{2} - \varphi \right)^{-1} + C_1, \end{aligned} \quad (A10)$$

where we only retain the divergent terms and the constant term C_1 , and accordingly,

$$\begin{aligned} \frac{d\tilde{\psi}}{d\varphi} \rightarrow & \frac{1}{2} \left(\frac{\alpha}{2} - C_2 \right) \left(\frac{d\tilde{h}}{d\varphi} \Big|_{\frac{\alpha}{2}} \right)^{-3} \left(\frac{\alpha}{2} - \varphi \right)^{-3} \\ & - \left(\frac{d\tilde{h}}{d\varphi} \Big|_{\frac{\alpha}{2}} \right)^{-3} \left(\frac{\alpha}{2} - \varphi \right)^{-2}. \end{aligned} \quad (A11)$$

In practice, the asymptotic forms (A10), (A11) can also be directly obtained by asymptotic analysis of Eq. (A4), without referring to its analytical solution. From the left side of Eq. (A4), we observe that the term $\frac{1}{h^3} \sim C(\frac{\alpha}{2} - \varphi)^{-3}$ determines the order of divergence of $\tilde{\psi}$ in the limit. Let $\tilde{\psi}$ have the asymptotic form $\tilde{\psi} \sim A(\frac{\alpha}{2} - \varphi)^{-B}$, then using this form in (A4), we have:

$$\begin{aligned} B(B+1)A \left(\frac{\alpha}{2} - \varphi \right)^{-B-2} - 3BA \left(\frac{\alpha}{2} - \varphi \right)^{-B-2} \\ + C \left(\frac{\alpha}{2} - \varphi \right)^{-3} = 0. \end{aligned} \quad (A12)$$

When $B = 1$, all the three terms on the left side of Eq. (A12) have the same order of divergence, and an algebraic equation follows to uniquely determine A . This

case corresponds to the term of lower order of divergence in (A9), (A10) and (A11) with determined coefficient $A = -1$. However, a higher order divergent term, which is not controlled by $\frac{1}{h^3}$, could also be present in the asymptotic solution. As for $B = 2$, the first two terms on the left side of Eq. (A12) cancel with each other, and A is left undetermined. This case corresponds to the arbitrary constant C_2 , which is associated with the term of higher order of divergence in (A9), (A10) and (A11).

Now it becomes immediately apparent that condition (A3) demands $C_2 = \frac{\alpha}{2}$, and only the first order divergence of $\tilde{\psi}$, which is always present, is allowed. Thus the problem to solve Eq. (19), together with boundary conditions (20), (A3) is complete, and unique solution $\tilde{\psi}$ exists for each value of the opening angle α .

In reflection, the physical content associated with boundary condition (A3) may invite further exposition. Taking into account of Eqs. (9) and (10), we note that boundary condition (A3) states physically $h\mathbf{v} = 0$ at contact lines. Consider the region with distance smaller than δ from the boundary. The influx $h\mathbf{v}$ should be in balance with the evaporation flux which is proportional to $J\delta$. Let δ go to 0, and our result follows. Mathematically, one can argue that in Eq. (19) the singular behavior or the order of divergence of $\tilde{\psi}$ in the limit $\varphi \rightarrow 0$ should be uniquely determined by the term $\frac{1}{h^3}$. The solution with higher order of divergence, though compatible with the mathematical structure, is not allowed by physics.

APPENDIX B: THE CROSSOVER AT THE 90-DEGREE OPENING ANGLE

It has been shown [5, 15], in the limit $r \ll R(t) \approx R_i$, the first two leading order terms in the full expansion of the surface height $h(t, r, \varphi)$ read as (for simplicity, we will replace $R(t)$ with R_i , and hence suppress the t dependence of h): for the opening angle $0 < \alpha < \pi$, and $\alpha \neq \frac{\pi}{2}$,

$$h(r, \varphi) = \frac{1}{4} \frac{r^2}{R_i} \left(\frac{\cos 2\varphi}{\cos \alpha} - 1 \right) + C \frac{r^{\frac{\pi}{\alpha}}}{R_i^{\frac{\pi}{\alpha}-1}} \cos \frac{\pi \varphi}{\alpha}; \quad (B1)$$

for $\alpha = \frac{\pi}{2}$,

$$h(r, \varphi) = -\frac{1}{\pi} \frac{r^2}{R_i} \ln \frac{r}{R_i} \cos 2\varphi + \frac{r^2}{R_i} \left(\frac{1}{\pi} \varphi \sin 2\varphi - \frac{1}{4} + C_0 \cos 2\varphi \right), \quad (B2)$$

where C and C_0 are related by (17), and C_0 is α independent.

As mentioned briefly before, the seeming divergence in (15), (16) and hence in (B1) at $\alpha = \frac{\pi}{2}$ is artificial as one can readily check by expanding those divergent terms in small parameter $(\frac{\pi}{2} - \alpha)$ near $\alpha = \frac{\pi}{2}$ as done in Refs 5 and 8, and $h(r, \varphi)$, if regarded as a function implicitly depending on α , is actually continuous at $\alpha = \frac{\pi}{2}$. What's more, as can be shown by the same method (we omit the

derivation here), all the derivatives of h with respect to r and φ up to any order are also continuous at $\alpha = \frac{\pi}{2}$.

As asymptotic approximation, we retained only the term of smaller exponents of r ($\frac{\pi}{\alpha} \leq 2$ according to $\alpha \geq \frac{\pi}{2}$) on the right side of (B1), treating $\alpha = \frac{\pi}{2}$ as the limiting case, even near $\alpha = \frac{\pi}{2}$ where the two terms become comparable to each other. Those approximations do bring about some subtleties on some occasions, and necessary corrections or modifications to our results obtained before need to be made.

In the case of velocity field, it was found in (33) that v_φ at contact lines would vanish in the limit $\alpha \rightarrow \frac{\pi}{2}$. However, intuitively according to the conservation of the fluid mass, velocity should be locally inversely proportional to the slope of the surface of the drop. As mentioned above, both $\frac{\partial h}{\partial r}$ and $\frac{\partial h}{\partial \varphi}$ remain finite, and are continuously dependent on the opening angle, even at $\alpha = \frac{\pi}{2}$, and therefore $v_\varphi|_{\alpha=\frac{\pi}{2}}$ should not be vanishing.

Really, in the first order correction, if we use instead the leading order term on the right side of (B2) i.e. $h(r, \varphi)|_{\alpha=\frac{\pi}{2}} = -\frac{1}{\pi} \frac{r^2}{R_i} \ln \frac{r}{R_i} \cos 2\varphi$ in (32) (that is, we approximate $\tilde{h}(\varphi)|_{\alpha=\frac{\pi}{2}}$ by $-\frac{1}{\pi} \ln \frac{r}{R_i} \cos 2\varphi$, and let $\nu = 2$), we obtain:

$$v_\varphi|_{\alpha=\frac{\pi}{2}} \rightarrow \frac{J_0}{\rho} \frac{\pi}{2} \left(\frac{r}{R_i} \right)^{-1} \left| \ln \frac{r}{R_i} \right|^{-1}, \quad (B3)$$

which is nonvanishing at contact lines.

Combining (33) and (B3), we realize that there is a

crossover in physics near the opening angle $\alpha = \frac{\pi}{2}$, which was somewhat concealed by the asymptotic analysis we employed in this paper, as well as in Ref. 6. We can actually estimate, though still crudely, the range $\Delta\alpha$ of the neighborhood near $\alpha = \frac{\pi}{2}$ where this crossover happens. We believe, as partly shown above, the velocity field (as well as all the physical properties of the system that we were considering in this paper and in Ref. 6) depends on the opening angle α continuously. And in the small neighborhood $[\frac{\pi}{2} - \Delta\alpha, \frac{\pi}{2} + \Delta\alpha]$ actual physics should be interpolated, so that (33), which only holds outside of the neighborhood, is related continuously to the result (B3), which applies exactly to $\alpha = \frac{\pi}{2}$. By comparing (33) with (B3), we find an estimate of $\Delta\alpha$ that follows from the condition:

$$\tan\left(\frac{\pi}{2} - \Delta\alpha\right) \approx \left| \ln \frac{r}{R_i} \right|, \quad (B4)$$

and therefore

$$\Delta\alpha \approx \frac{\pi}{2} - \arctan \left| \ln \frac{r}{R_i} \right| \approx \left| \ln \frac{r}{R_i} \right|^{-1}. \quad (B5)$$

In principle, all the results we've obtained so far, as well as those in Ref. 6 apply only outside of the neighborhood $[\frac{\pi}{2} - \Delta\alpha, \frac{\pi}{2} + \Delta\alpha]$.

[1] R. D. Deegan, O. Bakajin, T. F. Dupont, G. Huber, S. R. Nagel, T. A. Witten, *Nature*, **389**, 827 (1997).
[2] R. D. Deegan, *Ph.D. Thesis* (University of Chicago, Dept. of Physics, 1998).
[3] R. D. Deegan, O. Bakajin, T. F. Dupont, G. Huber, S. R. Nagel, T. A. Witten, *Phys. Rev. E* **62**, 756 (2000).
[4] R. D. Deegan, *Phys. Rev. E* **61**, 475 (2000).
[5] Y. O. Popov, T. A. Witten, *Eur. Phys. J. E* **6**, 211 (2001).
[6] Y. O. Popov, T. A. Witten, *Phys. Rev. E* **68**, 036306 (2003).
[7] Y. O. Popov, *Ph.D. Thesis* (University of Chicago, Dept. of Physics, 2003).
[8] N. D. Denkov, O. D. Velev, P. A. Kralchevsky, I. B. Ivanov, H. Yoshimura, K. Nagayama, *Langmuir* **8**, 3183 (1992).
[9] A. S. Dimitrov, C. D. Dushkin, H. Yoshimura, K. Nagayama, *Langmuir* **10**, 432 (1994).
[10] T. Ondarcuhu, C. Joachim, *Europhys. Lett.* **42**, 215 (1998).
[11] J. Boneberg, F. Burmeister, C. Shafle, P. Leiderer, D. Reim, A. Fery, S. Herminghaus, *Langmuir* **13**, 7080 (1997).
[12] R. G. Larson, T. T. Perkins, D. E. Smith, S. Chu, *Phys. Rev. E* **55**, 1794 (1997).
[13] O. B. Bakajin, T. A. J. Duke, C. F. Chou, S. S. Chan, R. H. Austin, E. C. Cox, *Phys. Rev. Lett.* **80**, 2737 (1998).
[14] C. C. Hsieh, L. Li, R. G. Larson, *J. Non-Newtonian Fluid Mech.* **113**, 147 (2003).
[15] H. K. Moffat, B. R. Duffy, *J. Fluid. Mech.* **96**, 299 (1979).
[16] S. Blume, M. Kirchner, *Optik* **29**, 185 (1969).